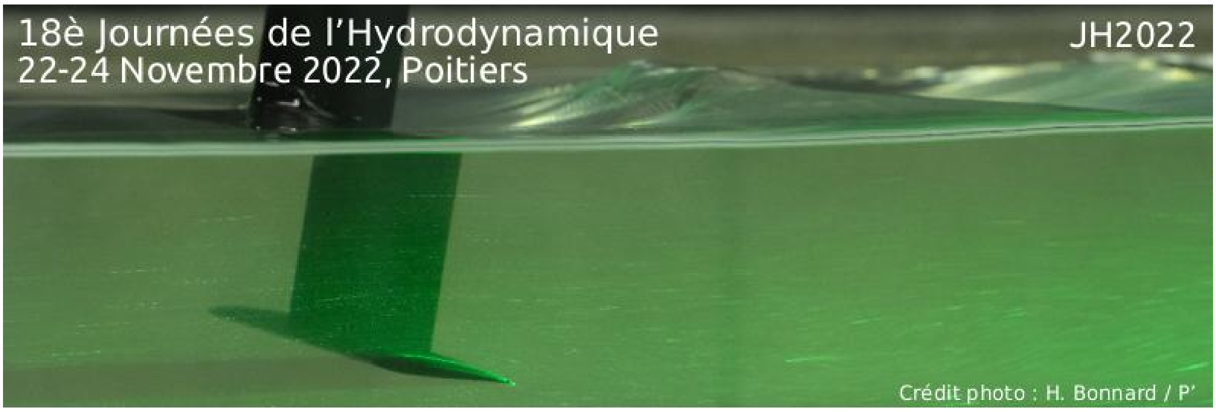

ÉTUDE EXPÉRIMENTALE D'UN HYDROFOIL PERÇANT UNE SURFACE LIBRE TRACTÉ DANS UN MILIEU VASEUX

EXPERIMENTAL STUDY OF A SURFACE-PIERCING HYDROFOIL TOWED THROUGH MUDDY ENVIRONMENTS

M. S. SOTELO[(1)], D. BOUCETTA[(1)], W. VAN HOYDONCK[(3)], M. VANTORRE[(1)], E. TOORMAN[(2)], G. DELEFORTRIE[(1)]

correspondance: marco.sotelo@ugent.be

[(1)] Maritime Technology Division, Ghent University, Ghent, Belgium
[(2)] Department of Civil Engineering, KU Leuven, Leuven, Belgium
[(3)] Flanders Hydraulics Research, Antwerp, Belgium

Résumé

Ce travail vise à fournir des données de validation pour les solveurs numériques destinés à modéliser le comportement des corps en mouvement dans des environnements vaseux réalistes. Une série d'essais de traction a été exécutée avec un hydrofoil dont le profil a une corde de 0.16 m, perçant la surface. A cet effet, l'influence du dégagement sous quille et l'influence de l'angle de dérive ont été prises en compte. Ces tests ont été effectués dans de l'eau douce, de l'eau de mer et de la vase naturelle provenant du port d'Anvers-Bruges. Les différents efforts hydrodynamiques ainsi que les mesures rhéologiques présentées dans ce travail peuvent être utilisées pour valider de nouveaux solveurs destinés à modéliser le comportement des fluides non newtoniens pour des applications nautiques.

Summary

This work aims to contribute with validation material for numerical solvers intended to model sailing bodies in realistic muddy environments. A series of towing tests with a 0.16 m chord surface-piercing hydrofoil were performed, including a variety of UKCs and drift angles. These tests were carried out in freshwater, seawater, and natural mud obtained from the Port of Antwerp-Bruges. The different hydrodynamic forces, and rheological measurements presented in this work can be used to validate new solvers intended to model non-Newtonian fluids for nautical applications.

I – Introduction

Many regions around the world have high deposition rates of cohesive sediments in their ports and waterways, affecting the maritime traffic [14]. In many cases, the accumulation of these sediments is the result of natural processes and its impact can be reduced by constant dredging. Nonetheless, the intrinsic cost associated with dredging operations had lead to the evaluation of safely sailing in muddy environments [27]. Several experimental and numerical studies have demonstrated that is possible so sail safely in these conditions without loosing the controllability of the vessel, even with the keel completely submerged in the mud layer [8]. However, these studies, mainly experimental, treated the mud layer as a Newtonian fluid, whereas in reality these sediments display a visco-plastic behaviour which is typically categorized as non-Newtonian fluids [1, 21].

With the rapid increase of computational power, Computational Fluid Dynamics (CFD) have become a popular method to perform ship hydrodynamics studies. Because of the difficulties of modelling the rheological properties, natural mud is frequently simplified as a Newtonian or a Bingham fluid. Even with such simplifications in the mud modelling, recent works based on CFD demonstrated to have an acceptable accuracy compared with experiments, as presented in [29, 10, 12]. However these models ignore the thixotropic behaviour of mud under accelerating or decelerating conditions. Therefore, more validation material is needed to fully test the capacity of CFD in realistic muddy environments.

Only a few works are known in literature dedicated to be used as validation material for CFD regarding mud modelling for nautical applications. In the work presented by [12], the authors performed towing experiments of a flat plate in natural mud. The results were compared with CFD simulations, demonstrating an acceptable agreement. Following the lessons learned from [23], in [19] the authors performed towing tests with a 0.2 m horizontal cylinder in a series of fluid combinations including freshwater, natural mud and seawater with natural mud. A significant influence of the water-mud interface in the hydrodynamic forces acting on the cylinder was reported. The experimental setup used in those tests was arranged in a way that a 2D condition can be assumed. For this reason, the current work aims to continue with the experiments of [19], by modifying the towed object to a 3D geometry. The selected towing object for this case is surface-piercing hydrofoil with a symmetrical NACA0015 profile.

Hydrofoils are devices used in many marine applications for commercial and recreational purposes. From high-speed sailing boats to open-water rudders or stabilizer bilge keels, hydrofoils are widely use as control or lifting devices. In the literature, many authors studied surface-piercing hydrofoils in freshwater at low-to-moderate draft-based Froude numbers $\left(Fr_T = U/\sqrt{gT}\right)$, which are typically comprised between $0.5 \lesssim Fr_T \lesssim 4$, according to [9, 28]. However, when navigating in muddy environments, different physics are involved that have not been investigated thoroughly before. The main purpose of this work is to study the behaviour of the hydrodynamic forces acting on a surface-piercing hydrofoil in realistic muddy environments, in low-to-moderate draft-based Froude numbers, for drift angles below stall. The different measurements presented in this work can be used as validation material for CFD models intended to be used in muddy environments. Currently a joint effort is made to use these measurements in the validation of the hybrid (fluid-sediment) two-phase/mixture CFD model [16] adapted for mud.

II – Methodology

II – 1 Experimental setup

Towing experiments with a surface-piercing hydrofoil were executed in the experimental facilities of Flanders Hydraulics Research (FHR) in Antwerp, Belgium. The flume tank is 20 m long, 0.56 m wide and 0.75 m deep. The object was towed steadily with a gear guided carriage, covering draft-based Froude numbers from 0 to 0.96. The hydrofoil was a NACA0015 profile with 0.16 m chord, 0.024 m thickness, 0.22 m total span, and was submerged 0.15 m (T) throughout the whole experimental program. The hydrofoil was tested at seven different drift angles, varying from -10, -5, -2.5, 0, 2.5, 5, and 10 degrees. A 6 DoF load cell was used to record the hydrodynamic forces and moments acting on the body at different drift angles. This load cell was located in the rod of the hydrofoil, 0.11 m above the free-surface, at 0.064 m (r) from the leading edge. The load cell is fixed to the hydrofoil and rotate to the desired drift angle. The global direction of the measured horizontal forces (X and Y) and yaw moment (N) are presented in Figure 1. In which the direction of the X force is parallel to the flume walls in the towing direction. The Z force is measured in the rod axis, pointing downwards. Four pressure probes were placed in the surface of the hydrofoil, at 0.05 m below the free-surface. Additionally, two sets of four pressure probes at different heights were placed at 5 and 10 m from the starting point, to generate pore pressure time series data at different depths, as indicated in Figure 1.

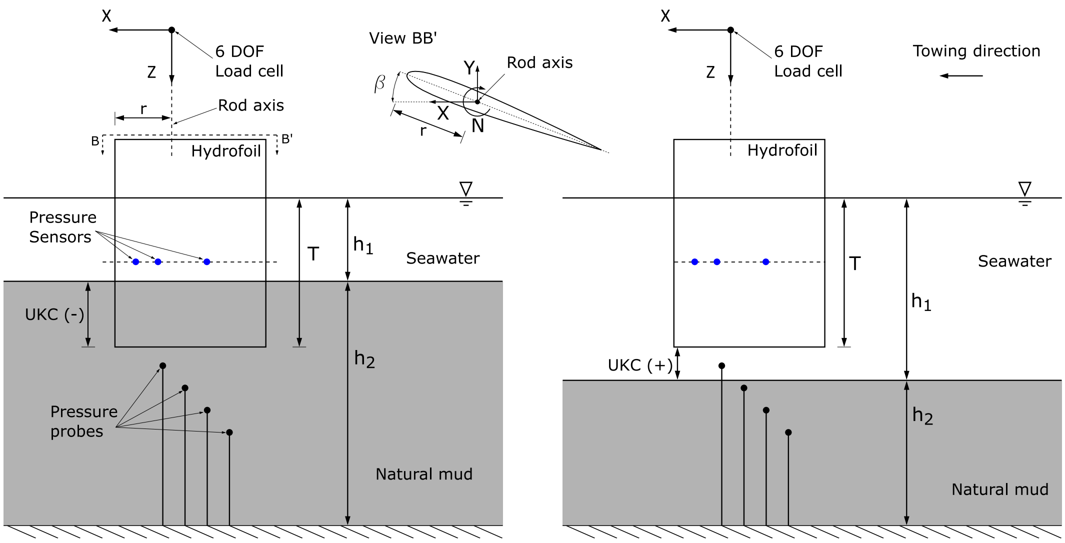

FIGURE 1 – Experimental arrangement and forces frame of reference

A variety of fluid combinations was considered in the test plan, including freshwater, natural mud and seawater with natural mud. A total of six under keel clearances ($UKC = (h_1 - T)/T$) were tested, including negative UKCs with respect to the mud layer (See Figure 1). For all the experiments, the total fluid level ($h_1 + h_2$) was kept at 0.508 m. To achieve the different UKCs in muddy environments, the seawater and natural mud layer thicknesses (h_1 and h_2 respectively) were varied accordingly as presented in Table 1. In conditions W to D, all seven drift angles were tested. For conditions E and F only three drift angles were included due to its similarity to the condition W (freshwater).

Table 1 – Experimental test series

		UKC $\left(\frac{h_1-T}{T}\right)$	h_1	h_2
Test name	Fluid	$[\%T]$	$[m]$	$[m]$
W	Freshwater	-	0.508	-
A	Mud	-100	-	0.508
B	SW* and mud	-50	0.075	0.433
C	SW* and mud	-25	0.1125	0.3955
D	SW* and mud	0	0.15	0.358
E	SW* and mud	+25	0.1875	0.3205
F	SW* and mud	+50	0.225	0.283

SW* : seawater

All the raw signals coming from the load cell and pressure sensors were post-processed using a low-pass filter. A threshold of 10 Hz was imposed, which is the expected frequency band-width to which the different phenomena are expected to occur. To estimate the uncertainty of the mean value the RUM method was used [4]. Some of the results of the force measurements will be included in the following sections.

II – 2 Mud handling and rheological parameters

The natural mud and seawater including in these experiments were obtained from the Zeebrugge outer harbour area (Port of Antwerp-Bruges). The natural mud was kept in a dark reservoir to prevent excessive oxidation due to UV light. A pitched impeller mixer was used to condition the mud, before every day of tests, to ensure the homogeneity of the fluid. Once the conditioning was ready, it was poured into the flume to the desired level, and subsequently covered with the seawater in the required conditions. As the degradation of organic matter can affect the properties of natural slurries [13], a verification of the rheological parameters was performed every test day. Measurements of the mud profile with a gamma-densitometer were also included, which displayed a constant trend of the density profile along the mud layer, indicating a desired level of homogeneity. The rheological properties of the mud layer were obtained using the protocol described in [5], and characterized with the four parameter Worrall-Tulliani model [26], which has the following form :

$$\tau = \tau_y + \mu_\infty \dot{\gamma} + \frac{(\mu_0 - \mu_\infty)\dot{\gamma}}{1 + \left(\frac{\mu_0 - \mu_\infty}{\tau_B - \tau_y}\right)\dot{\gamma}} \tag{1}$$

In eq. 1 τ_y represents the true yield stress, τ_B is the Bingham stress, μ_0 is the differential initial viscosity, and μ_∞ is the Bingham viscosity. This model was used to fit the rheometer data corresponding to the tested natural mud, using Toorman's iterative method [20]. The different rheological characteristics of the tested fluids based on the Worrall-Tulliani model are presented in Table 2.

Table 2 – Main characteristics of the tested fluids

	Density	Viscosity	Worrall-Tulliani coefficients			
	ρ	μ	μ_∞	μ_0	τ_Y	τ_B
Fluid	$[kg/m^3]$	$[Pa.s]$	$[Pa.s]$	$[Pa.s]$	$[Pa]$	$[Pa]$
Freshwater	1000	1.00e-3	-	-	-	-
Seawater	1020	1.07e-3	-	-	-	-
Natural mud	1176.1	-	0.0091	1.50	3.25	5.08

III – Experimental results and discussion

III – 1 Results in freshwater

Initial test in freshwater were performed to have a general overview of the magnitude and tendencies of the hydrodynamic forces acting on the hydrofoil. The tests were executed covering a range of draft-based Froude number from 0 to 0.96. During these tests a significant deformation of the free-surface occurs as the velocity increased, see Figure 2.

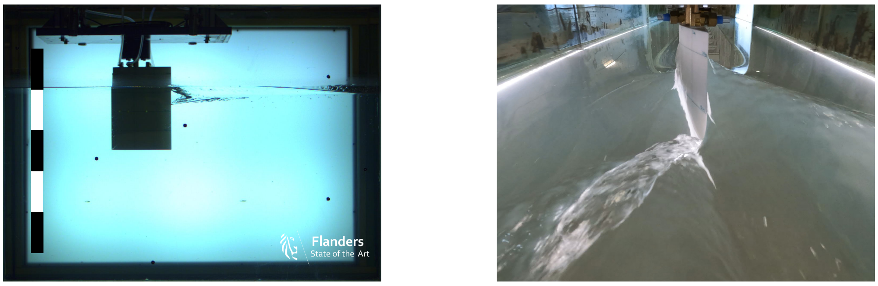

Figure 2 – Test in freshwater at $\beta = -10°$, $Fr_T = 0.96$

The forces and yaw moment acting on the X-Y plane are presented in Figure 3. The non-dimensional coefficients were calculated using the common definitions :

$$C_X = \frac{|X|}{0.5\rho A U^2};\ C_Y = \frac{|Y|}{0.5\rho A U^2};\ C_N = \frac{|N|}{0.5 r\rho A U^2} \tag{2}$$

Where A is the wetted surface of the hydrofoil, ρ the fluid density, U the velocity of the carriage and for the drift coefficient r is the position of the rod from the leading edge ($r = 0.064m$).

The measured hydrodynamic forces presented in Figure 3 display a undulating tendency that could be attributed to different sources. Contrary to the expected quadratic relationship with the velocity, the forces displayed an inflection point followed by a plateau in their tendencies, at low drift angles. It is known that partial ventilation could drastically affect the performance of piercing hydrofoils at low and moderate Froude numbers at drift angles below the stall [9]. For some critical conditions tested in this work, partial ventilation could appear as one stable regime, according to [28]. However, during the towing tests, only a fully wet condition was observed but not partial ventilation. What is displayed in Figure 2 is a large deformation of the free-surface, but not air entering towards the suction face of the hydrofoil. The fully wet condition was observed for all different cases including seawater and mud experiments. Another potential cause of these unexpected tendencies in the measured forces was the confinement of the experiment.

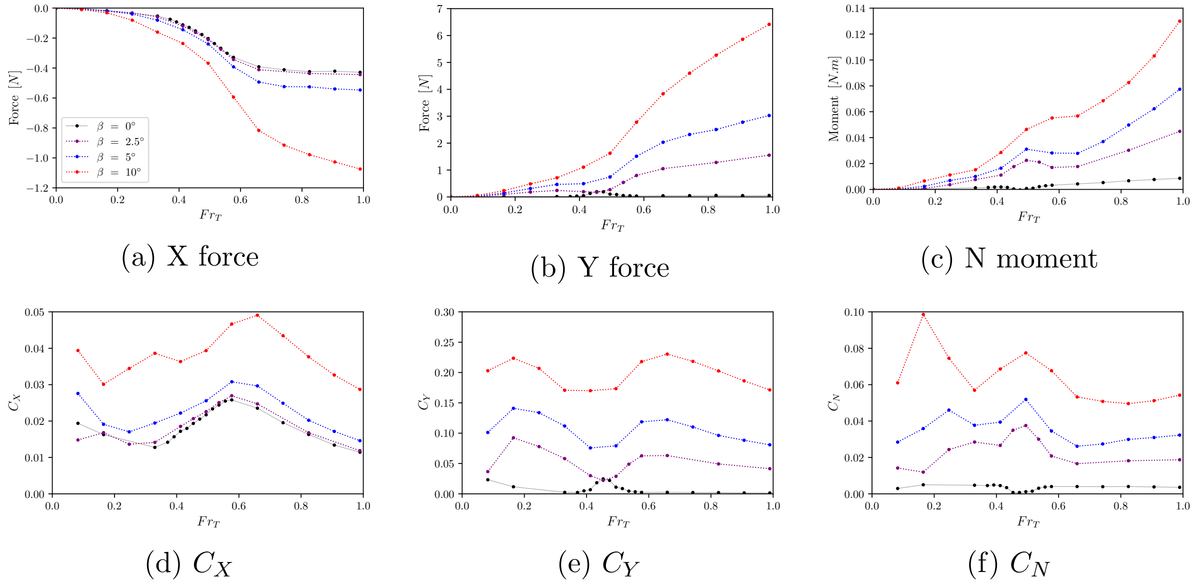

(a) X force (b) Y force (c) N moment

(d) C_X (e) C_Y (f) C_N

FIGURE 3 – Hydrodynamic forces and coefficients acting on the hydrofoil in water.

This was checked based on the criteria posed in [17], with which it was found that the blockage coefficient of the experimental setup was low enough and could thus not affect the experimental results. Hence, the non-uniform tendencies of the measured forces have a different source.

The X force in particular displays a rapid increment at Fr_T close to 0.4, until reaching a plateau at about $Fr_T = 0.7$, at low drift angles ($\beta \leq 5°$). The value of $Fr_T = 0.4$ is close to the so-called "Hull-speed" ($Fr_L \approx 0.4$), that is the velocity for which the transverse generated wave is equal to the length of the moving object. As the length (chord) in this case is about equal to the draft, Fr_T and Fr_L are about equal too, but not in general. For $Fr_T > 0.6$ a negative interaction between the bow wave with the stern wave system, can explain the constant tendency in the horizontal force [11]. It can be noticed that this tendency is only present at low drift angles. Once the drift angle increases, the transverse wave generated in the bow is not longer symmetrical, hence the interaction with the stern wave system has a lower effect on the X force. The influence of the drift angle in the X force can be observed in Figure 3.(a), in which at $\beta = 10°$, the inflection point was shifted to a higher Fr_T, and the plateau is not reached.

An inflection in the Y force and yaw moment tendencies for the drift angles tested was also observed around a same Fr_T range. Similarly to the X force, the negative interaction of the two wave systems influence the overall forces in the X-Y plane. This explains the undulating tendency in the non-dimensional coefficients presented in Figure 3. The non-zero yaw moment and Y force could be related to a small misalignment in the experimental setup, which will be taking into account in future works.

III – 2 Results in muddy environments

III – 2.1 Condition A, single interface in natural mud

Following with the experimental program, series of towing tests were executed in natural mud. The same range of Fr_T and drift angles as in the case of freshwater were tested. Many similarities are shared with the previous tests in freshwater since both were single interface scenarios. An example of a test in natural mud is presented in Figure 4. Large deformations of the free-surface were observed at high Fr_T. Nonetheless, the generated wake was rapidly attenuated due to the high viscosity of the natural mud. Even if the opacity of the fluid would allow it, no signs of partial ventilation were observed during this condition.

FIGURE 4 – Experiment in condition A at $Fr_T = 0.96$, $\beta = 5°$ (left), and $\beta = -5°$ (right)

Figure 5 shows the forces acting on the hydrofoil in condition A, for the whole velocity range. In the same manner as the freshwater case, only the forces acting on the X-Y plane are presented. To avoid issues with non-dimensional coefficients at $Fr_T \approx 0$, the initial measurement was excluded from the calculation, using the following expressions :

$$C'_X = \frac{|X - X_0|}{0.5\rho A U^2};\ C'_Y = \frac{|Y - Y_0|}{0.5\rho A U^2};\ C'_N = \frac{|N - N_0|}{0.5 r \rho A U^2} \tag{3}$$

Where X_0, Y_0 and N_0 represent the forces X and Y and the yaw moment respectively, measured at $Fr_T \approx 0$.

A non-zero value for X and Y forces at velocities close to zero can be observed, for all drift angles tested. This initial value is related to the yield stress, which is an important rheological characteristics of natural mud for nautical applications [22]. Some authors interpret this property as an initial rigidity that needs to be overcome for the mud layer flow. This definition is still debatable from a rheological point of view, but can be considered as adequate within the confines of this project [2]. Similar observations for a horizontal cylinder were reported in [19]. The yield stress not only affects the longitudinal, but also the lateral force, at non-zero drift angles.

Apart from the yield stress influence at low speed, the overall tendency of the forces are quite similar to the freshwater case. The inflexion points observed before are also present in this condition, however its effect seems to be attenuated. This could be due to the high viscosity of the mud layer that tends to damped the generated waves, reducing drastically the interaction between them. The yaw moment at non-zero drift angles has negative value at low speeds. This is an indication of the change in the location of the lateral centre of pressure with the velocity, which could also be related to the yield stress.

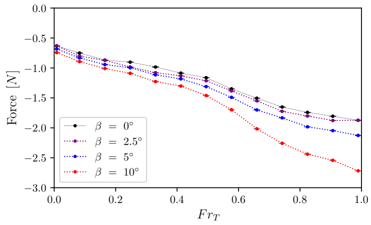

(a) X force

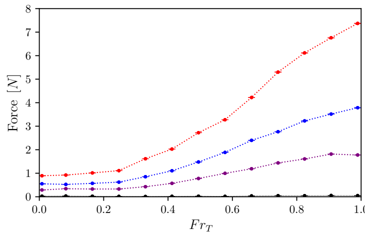

(b) Y force

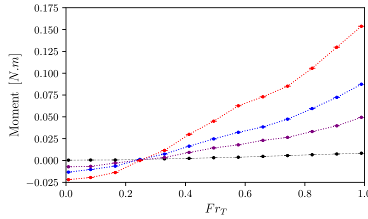

(c) N moment

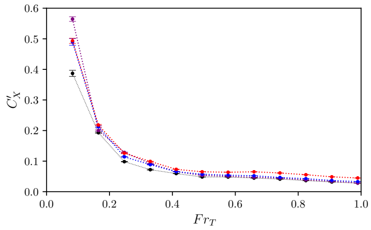

(d) C'_X

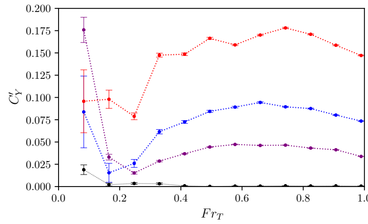

(e) C'_Y

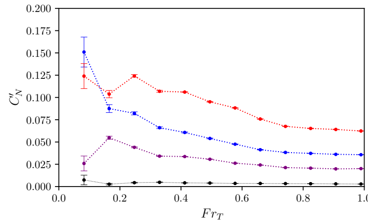

(f) C'_N

FIGURE 5 – Hydrodynamic forces and coefficients acting on the hydrofoil in natural mud.

III – 2.2 Tests in seawater and natural mud

In more realistic muddy environments, vessels navigate in a layered fluid composed by seawater and natural mud. To replicate this realistic scenario, towing experiments were conducted in seawater and natural mud, including different UKCs with respect to the mud layer. To have a fair comparison, the same range of velocities and drift angles were tested as the previous cases. An example of these tests are presented in Figure 6.

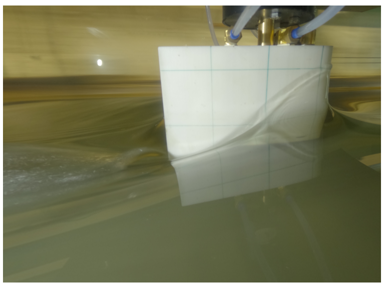
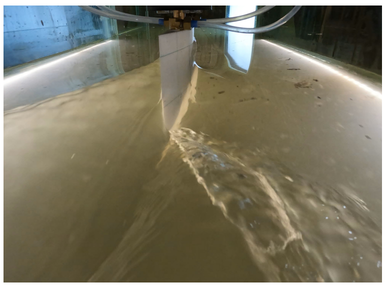

FIGURE 6 – Tests in condition B ($-50\%\ UKC$), at $\beta° = 10$ and $Fr_T = 0.96$

In Figure 6 the most critical case included in this section of the experimental phase is displayed. In these conditions, no signs of partial ventilation were observed. Only a significant deformation of the free-surface, as presented previously for the other tested fluids was observed. Under this condition, the interface between the seawater and natural mud was expected to deform significantly, as in the case for ship models [24, 6], however, that was not the case. In Figure 7 a side view of the experiments on each condition for the highest critical velocity and drift angle are presented.

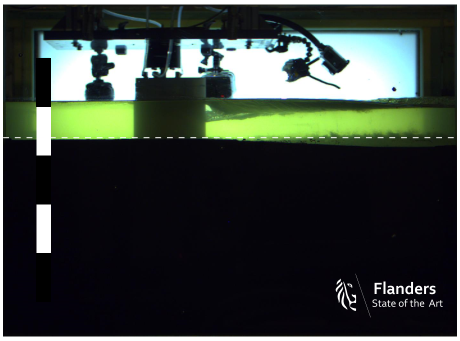

(a) Condition B at $\beta = 10°$, $Fr_T = 0.96$

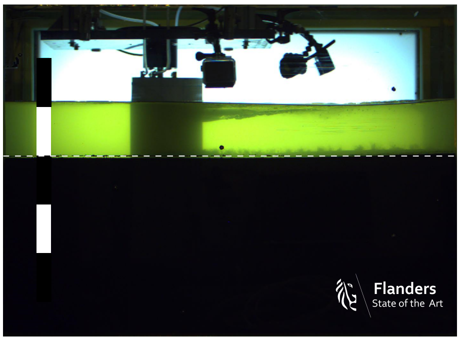

(b) Condition C at $\beta = 10°$, $Fr_T = 0.96$

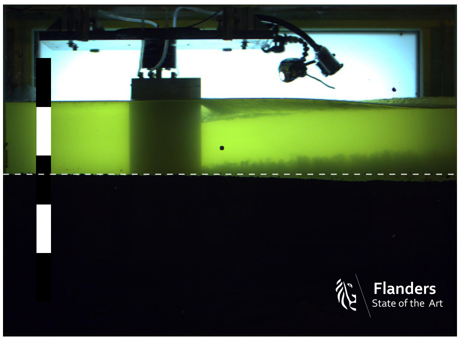

(c) Condition D at $\beta = 10°$, $Fr_T = 0.96$

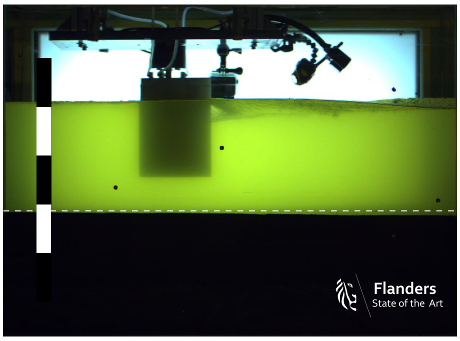

(d) Condition E at $\beta = 10°$, $Fr_T = 0.96$

FIGURE 7 – Tests in seawater and natural mud. The dashed white line indicates the initial mud level on each condition

Undulations of the water-mud interface were observed at negative to zero UKCs, for the highest Fr_T and drift angles tested, as displayed in Figure 7. These undulations were also seen at mid-velocities, although they were smaller. For low Fr_T almost no undulations or perturbations were observed in the water-mud interface. In tests with positive UKC, almost no undulations in the water-mud interface were observed. For tests with negative to zero UKC, the wake generated by the hydrofoil was followed by a turbid cloud of eroded sediments from the upper section of the mud layer. This turbid portion of the wake was most notorious in condition D, in which the bottom face of the hydrofoil was in contact with the upper section of the mud layer, disturbing it more comparing to the negative UKC cases. The upper section of the mud layer was mainly composed by loose particles and an oxidised layer of the mud.

Surface waves generated by moving bodies on a fluid can be related to the pressure disturbances. In the free-surface, since the density ratio is large, small perturbations can generate wave systems. Internal waves on the other hand, normally have low frequencies due to the small density ratio [15]. For the case of the water-mud experiments, the density ratio between both fluids is about 17%. Moreover, the slenderness of the hydrofoil is large enough so that its motion in the mud layer does not generate sufficient disturbance to produce a significant wake. The blockage of the experiment does not play a role in the formation of internal waves in this case, because undulations in towing tank experiments were reported in previous works in natural and artificial mud [3, 25, 18, 7]. It is known that undulations in the water-mud interface have a significant influence on the hydrodynamic forces acting on the body. To have a better comparison among all the tested cases, in Figure 5 all conditions at $\beta = 10°$ are presented.

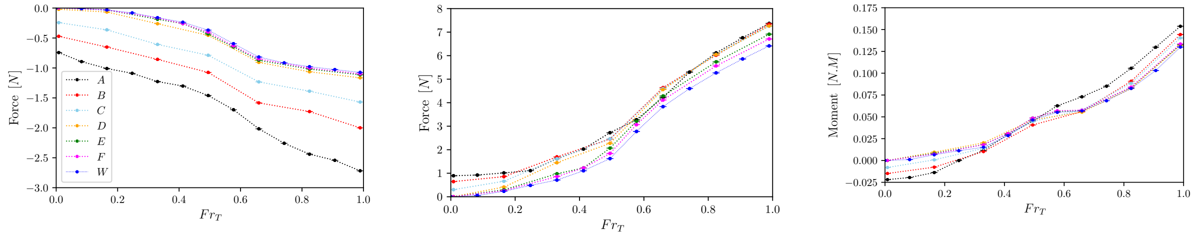

(a) X force

(b) Y force

(c) N moment

FIGURE 8 – Comparison measurements in all tested conditions at $\beta = 10°$

For water-mud cases, it was not possible to calculate the non-dimensional coefficient using the general definition presented in equation 2. However, in the literature more suitable non-dimensional coefficients have been proposed for visco-plastic fluids, but this is left for future work. The overall magnitudes of the forces and yaw moment acting on the X-Y plane have an increasing tendency with Fr_T. In Figure 8.(a), one can observe the influence of the yield stress for the negative UKC cases. This influence seems to be reduced in the same proportion as the UKC with the mud layer. It is also worth mentioning that the magnitude of the X force, which can be directly related to the drag, is significantly larger compared to the freshwater case, even if the density difference between both fluids is about 17%. This is due to the influence of the rheological properties of the natural mud layer.

Another observation from the measurements presented in Figure 8 is that both forces X and Y do not display a significant variation once the hydrofoil is no longer in contact with the mud layer. This effect is most visible in Figure 8.(a). The lateral force Y is also affected by the presence of the mud layer, however in less proportion than in the case of freshwater. The intermediate cases of negative UKCs fall in between the case with freshwater and mud only, similarly to the X force.

IV – Conclusions

A series of towing tests have been conducted in muddy environments to study the hydrodynamic forces acting on a 0.16 m chord surface-piercing hydrofoil at low-to-moderate Froude numbers. Different measurements indicate that there is a significant influence of the mud layer on the hydrodynamic forces, particularly when the body is completely or partially submerged in the mud layer.

Initial towing tests in freshwater demonstrated positive and negative interactions between the bow and stern wave systems for $Fr_T > 0.4$. These interactions modified the force magnitude parallel to the movement of the object. This interaction was reduced with the increment of the drift angle, due to an induced asymmetry in the wave systems.

In cases with negative UKCs (-100, -50 and -25%), the influence of the yield stress is present in the measured forces, especially in the X direction. Due to the visco-plastic nature of the natural mud and its high viscosity, the wake generated by the hydrofoil is rapidly attenuated, reducing the positive and negative interaction of the bow and stern wave systems.

Small undulations in the water-mud interface were observed, compared to similar ship model tests. This is due to slenderness of the hydrofoil and the small pressure variation in the water-mud interface generated by the moving object. The undulations observed during the experiments were rapidly attenuated.

V – Acknowledgment

The authors would like to thank Flanders Hydraulics Research for the continuous collaboration during the experimental campaign. Moreover, the research in this paper is funded by Research Foundation - Flanders, grant G0D5319N.

References

[1] H. Barnes, F. Hutton, and K. Walters. An introduction to rheology. *Polymer*, 31(4) :766, April 1989.

[2] H. A. Barnes. The yield stress-a review or '$\pi\alpha\nu\tau\alpha\ \rho\epsilon\iota$'-everything flows ? *Journal of Non-Newtonian Fluid Mechanics*, 81(1-2) :133–178, feb 1999.

[3] C. Brossard, A. Delouis, P. Galichon, J. Granboulan, and P. Monadier. Navigability in channels subject to siltation physical scale model experiments. *Coastal Engineering 1990*, 3 :3088–3101, 5 1990.

[4] J. Brouwer, J. Tukker, Y. Klinkenberg, and M. van Rijsbergen. Random uncertainty of statistical moments in testing : Mean. *Ocean Engineering*, 182 :563–576, 2019.

[5] S. Claeys, P. Staelens, J. Vanlede, M. Heredia, T. van Hoestenberghe, T. van Oyen, and E. Toorman. A rheological lab measurement protocol for cohesive sediment. In *13th International Conference on Cohesive Sediment Transport Processes*, 2015.

[6] G. Delefortrie. *Manoeuvring Behaviour of Container Vessels in Muddy Navigation Areas*. PhD Thesis, Ghent University, 2007.

[7] G. Delefortrie, M. Vantorre, and K. Eloot. Modelling navigation in muddy areas through captive model tests. *Journal of Marine Science and Technology*, 10(4) :188–202, 2005.

[8] G. Delefortrie, M. Vantorre, E. Verzhbitskaya, and K. Seynaeve. Evaluation of safety of navigation in muddy areas through real-time maneuvering simulation. *Journal of Waterway, Port, Coastal and Ocean Engineering*, 133(2) :125–135, mar 2007.

[9] C. M. Harwood, Y. L. Young, and S. L. Ceccio. Ventilated cavities on a surface-piercing hydrofoil at moderate froude numbers : Cavity formation, elimination and stability. *Journal of Fluid Mechanics*, 800 :5–56, 8 2016.

[10] S. Kaidi, E. Lefrançois, and H. Smaoui. Numerical modelling of the muddy layer effect on ship's resistance and squat. *Ocean Engineering*, 199 :106939, 3 2020.

[11] L. Larsson, H. C. Raven, and J. R. Paulling. *Principles of Naval Architecture : Ship resistance and flow*. Society of Naval Architects and Marine Engineers, 2010.

[12] S. Lovato, A. Kirichek, S. Toxopeus, J. Settels, and G. Keetels. Validation of the resistance of a plate moving through mud : CFD modelling and towing tank experiments. *Ocean Engineering*, 258 :111632, aug 2022.

[13] W. Markgraf, C. W. Watts, W. R. Whalley, T. Hrkac, and R. Horn. Influence of organic matter on rheological properties of soil. *Applied Clay Science*, 64 :25–33, 2012.

[14] W. H. McAnally, A. Teeter, D. Schoellhamer, C. Friedrichs, D. Hamilton, E. Hayter, P. Shrestha, H. Rodriguez, A. Sheremet, and R. Kirby. Management of Fluid Mud in Estuaries, Bays, and Lakes. II : Measurement, Modeling, and Management. *Journal of Hydraulic Engineering*, 2007.

[15] J. N. Newman. *Marine Hydrodynamics*. The MIT Press, 40th anniv edition, 2018.

[16] M. Ouda and E. A. Toorman. Development of a new multiphase sediment transport model for free surface flows. *International Journal of Multiphase Flow*, 117 :81–102, 2019.

[17] J. B. Schijf. Protection of embankments and bed in inland and maritime waters, and in overflows or weirs. In *PIANC 17th congress, Section SI C2*, pages 1–18, 1949.

[18] R. Sellmeijer and G. Oortmerssen. The effect of mud on tanker manoeuvres. *Royal Institution of Naval Architects*, 1983.

[19] M. S. Sotelo, D. Boucetta, G. Delefortrie, E. Toorman, and D. Praveen. Experimental study of a cylinder towed through nautural mud. In *6th MASHCON*, Glasgow, Scothland, 2022.

[20] E. Toorman. An analytical solution for the velocity and shear rate distribution of non-ideal Bingham fluids in concentric cylinder viscometers. *Rheologica Acta*, 33(3) :193–202, 1994.

[21] E. Toorman. Modelling the thixotropic behaviour of dense cohesive sediment suspensions. *Rheologica Acta*, 36(1) :56–65, 1997.

[22] E. Toorman, M. Liste, M. Heredia, I. Rocabado, J. Vanlede, G. Delefortrie, T. Verwaest, and F. Mostaert. CFD Nautical Bottom : Rheology of fluid mud and its modeling, Feasibility Study. WL Rapporten 00_048, Flanders Hydraulics Research and KUL Leuven Hydraulics Laboratory and Antea Group, 2014.

[23] E. Toorman, I. Vandebeek, M. Liste Muñoz, M. Heredia, I. Rocabado, J. Vanlede, G. Delefortrie, M. Vantorre, and Y. Meersschaut. Drag on an object towed through a fluid mud layer : CFD versus experiment. *INTERCOH2015 : 13th International Conference on Cohesive Sediment Transport Processes. Leuven, Belgium, 7-11 September 2015*, 74(1997) :114–115, 2015.

[24] M. Vantorre. Ship behaviour and control at low speed in layered fluids. In *International Symposium on Hydro- and Aerodynamics in Marine Engineering (HADMAR), BSHC*, Varna, Bulgaria, 1991.

[25] M. Vantorre and I. Coen. On sinkage and trim of vessels navigating above a mud layer. In *9th International Harbour Congress, V.II KVIV*, 1988.

[26] W. Worrall and S. Tuliani. Viscosity changes during the ageing of clay-water suspensions. *Trans. Brit. Ceramic Soc.*, 63 :167–185, 1964.

[27] R. W. Wurpts. 15 years experience with fluid mud : Definition of the nautical bottom with rheological parameters. *Terra et Aqua*, (99) :22–32, 2005.

[28] Y. L. Young, C. M. Harwood, F. M. Montero, J. C. Ward, and S. L. Ceccio. Ventilation of lifting bodies : Review of the physics and discussion of scaling effects. *Applied Mechanics Reviews*, 69, January 2017.

[29] G. Zhiliang, Y. Hua, and X. Mingxiao. Computation of flow around wigley hull in shallow water with muddy seabed. *Journal of Coastal Research*, pages 490–495, 2015.